Forestry *An International Journal of Forest Research*

Institute of Chartered Foresters

# When economically optimal is ecologically complicated: modeling tree-by-tree cutting decisions to maximize financial returns from northern hardwood stands

**John D. Foppert[1,2*] and Neal F. Maker[3]**

[1]*Department of Forestry, Paul Smith's College, 7777 State Rte. 30, Paul Smiths, NY, 12981, USA*

[2]*Institute of Forest Economics, Technical University of Munich, Hans-Carl-von-Carlowitz-Platz 2, D-85354 Freising, Germany*

[3]*Forest Biometrics Research Institute, 4033 SW Canyon Road, Portland, OR, 97221, USA*

*Corresponding author: Tel: +1 518 327 6376; Email: jfoppert@paulsmiths.edu

This study challenges a long-standing and often uncontested assertion in the forestry discourse that maximizing financial returns always requires ecologically simplified stands. We developed a high-resolution simulation tool for northern hardwood stands in eastern North America and integrated advanced numerical optimization methods to model the tree-level harvest decisions that maximize financial returns. We modeled each individual tree's growth and its probability of natural mortality, conditioned on the evolving neighborhood-scale competitive environment it resides in. We developed size-, species-, and grade-specific price functions to assign potential harvest revenue values to each discrete bole section of each standing tree, and we used an evolutionary search algorithm to specify the financially optimal timing of tree-by-tree removals. We modeled three different case studies, representing a broad range of northern hardwood stand conditions, including a hypothetical 50-year-old, even-aged stand and two inventoried stands in northern New York, USA with contrasting management histories. We observed consistent results across all three cases: maximizing financial returns from northern hardwood forests requires silvicultural finesse and results in ecologically complicated stands.

## Introduction

It is often assumed that forests managed to maximize financial returns simply *must* be uniform, monocultural, and, in some general sense, ecologically disinteresting. Conversely, ecologically rich forests simply *must* underperform financially. Palik et al. (2021), for example, assert that simplified age- and size-class structure is a "nearly universal outcome of timber-focused silviculture" (p. 295), and Himes et al. (2022) refer to the "substantially lower financial returns" (p. 2) associated with silvicultural practices that create complex stands. Here, we examine those assumptions as they apply to northern hardwood forests in eastern North America.

Fostering within-stand structural complexity is a key objective of "ecological" and "closer-to-nature" approaches to forest management (Franklin et al., 2018; Larsen et al., 2022) and numerous silvicultural strategies have been developed specifically to enhance structural complexity (Seymour et al., 2002; Schutz, 2002; Graham and Jain, 2005; Raymond et al., 2009). We approached the subject of ecological complexity in managed forests from a different direction. We aimed to model financially optimized silviculture, without limiting cutting choices to a menu of standard silvicultural treatments (cf Pauwels et al., 2007; Stout and Brose, 2014; Meek and Lussier, 2014; Labelle et al., 2018), and then to observe the ecological structure of the resulting stands. What patterns would emerge if economically optimal harvesting decisions were modeled without constraints on the complexity of the silviculture employed?

Ashton and Kelty (2018) refer to regeneration and tending as the "two broad categories" of silvicultural treatments (p. 30). A silvicultural system results from the arrangement of such treatments within a stand, their timing across a sequence of entries, and the specific patterns of removal they prescribe. In order to accommodate irregular management and stand structures, it is therefore necessary for models of stand development to account for regeneration and tending at sub-stand scales, allowing both to be carried out at different times in different areas, and accurately projecting residual growth and regeneration responses. Attempts to optimize management must quantify the payoffs that result from various combinations of treatments.

Regeneration is perhaps the more studied of the two treatment types. Contemporary silviculturalists devote considerable attention to novel regeneration strategies (D'Amato et al., 2018; Achim et al., 2022) and forest economists continue to probe rotation-ending "optimal stopping" problems (Newmann, 2002; Kant, 2013). Close examination of tending decisions has proven more challenging and has attracted less attention (Hyytiäinen and Tahvonen, 2002; Parkatti and Tahvonen, 2020). This stems from the difficulty of both projecting growth responses to partial cutting and solving multi-dimensional optimization problems.

However, thanks to steady advances in growth modeling (Assmann, 1970; Ek et al., 1988; Weiskittel et al., 2011; Mäkelä and Valentine, 2020) simulation tools can provide increasingly accurate predictions of thinning responses to dynamic cutting treatments. And recent advances in numerical methods have opened the door to integrating these complex biometric models into rigorous economic analysis. The modern ecologic-economic optimization approach, sometimes referred to as the "Helsinki School" of resource economics (e.g. Tahvonen and Salo, 1999; Tahvonen and Rämö, 2016; Assmuth et al., 2021), has provided a successful framework for pairing sophisticated "abstract

economic models of optimization and ecological models of population growth" (MacLeod and Nagatsu, 2016, p. 420).

In forestry, the main line of that tradition operates primarily at the stand scale, using size-class-level harvest percentages as the control variable (e.g. Tahvonen et al., 2010). The Nordic forests for which this approach was initially developed typically have more species diversity and a broader distribution of size classes than monocultural plantations but are still simple enough in terms of stand structure and quality differentiation to be effectively managed with uniform silvicultural treatments. Nordic thinning strategies are thus more complex than the geometric methods employed in plantations. Thinning intensity varies among size classes and between time periods, but nevertheless results in relatively homogeneous composition, density, and structure within a stand (Hyytiäinen and Tahvonen, 2002).

Optimizing thinning through size-class harvest vectors may be less well suited for more complex stands, especially where stem quality is highly differentiated. When significant variability exists within stands and between individual trees, predicting tree growth from stand-level attributes and restricting optimal harvesting choices to uniformly applied treatments can introduce substantial aggregation errors in the analysis (Foppert, 2019). Alternatively, tree-level harvest optimization is an emerging trend in the forest management and economics literature (Härtl et al., 2010; Coordes, 2014; Vauhkonen and Pukkala, 2016; West et al., 2021; Sun et al., 2022; Koster and Fuchs, 2022). These methods can accommodate mixed-species stands (Bettinger and Tang, 2015; Dong et al., 2020; Dong et al., 2022) and those with complex structure (Frannson et al., 2020; Pascual, 2021; Pascual and Guerra-Hernández, 2022) or widely varied individual-tree quality (Meilby and Nord-Larsen, 2012; Foppert, 2019; Lohmander, 2019; Foppert, 2022).

Tree-level optimization builds on a rich history of individual-based modeling in forest ecology (see Pommerening and Grabarnik, 2019) which has had applications across spatial scales and forest types (e.g. Botkin et al., 1972; Mitchell, 1975; Shugart, 1984; Pacala et al., 1993). Pommerening and Grabarnik (2019) describe individual-based ecology as "a strict bottom-up approach, where system properties are derived from the interactions between individuals [i.e. trees] constituting these systems" (p. 1). Most (but not all) tree-level optimization studies work within an individual-based modeling framework to represent competition and tree growth.

As an emerging area of research, many gaps exist in the tree-level optimization literature. Accounting for natural mortality remains a challenge. Many studies simply assume mortality away, either explicitly (e.g. Meilby and Nord-Larsen, 2012; Koster and Fuchs, 2022) or implicitly (e.g. Lohmander, 2019; West et al., 2021; Foppert, 2022). Frannson et al. (2020) employed a deterministic procedure to account for mortality from self-thinning, though this only describes a subset of all the ways a tree can die (Anderegg et al., 2015; Das et al, 2016). Sun et al. (2022) treated survival as a stochastic process but used arbitrarily drawn thresholds to trigger individual-tree mortality.

Another challenge relates to the exponential nature of individual-tree selection as a combinatorial problem. In even just a modest sized stand, the solution space for a tree-level optimization problem is overwhelmingly large (Foppert, 2019). Different studies confront this challenge in different ways, but a common approach is to restrict analysis to just a single plot (e.g. Härtl et al., 2010; Koster and Fuchs, 2022; Sun et al., 2022). These studies focus their attention on the complex mechanics of optimal thinning, but they provide no visibility into emergent stand-level

cutting patterns. This significantly limits their application outside of uniform silvicultural systems, where neighborhood structure and the proportion and arrangement of regeneration treatments within a stand play a critical role (Raymond et al., 2009; Labelle et al., 2018).

The primary objective of this study was to develop a method for defining financially optimal individual-tree harvest schedules for complex northern hardwood stands. Secondarily, we sought to observe the projected ecological structure of those stands resulting from that management. The remainder of this paper is structured as follows: the next section presents the theoretical model and the numerical simulation and optimization methods; the following section introduces the case studies; a fourth section presents the results; a fifth section offers a discussion; and the final section concludes.

## Materials and methods

### *Theoretical model*

Consider a silvicultural strategy which conceptualizes a forest stand as a mosaic of independent neighborhoods, where a neighborhood is an area sufficiently small that all of the trees within it interact in a nearly homogeneous competitive environment but sufficiently large that neighborhood-level summary statistics accurately describe that environment. That is, a neighborhood must not be so large that substantial environmental variation exists within it, but not so small that its environment is significantly (and unaccountably) influenced by trees outside of it. Functionally, a neighborhood should be large enough to accommodate two or three trees of end-of-rotation stature. Target crop tree densities of 150-175 $tr \cdot ha^{-1}$ (e.g. Miller et al, 2007) imply neighborhoods in the range of 0.01-0.02 ha, consistent with how the neighborhood concept has been operationalized in the ecology literature (Canham and Uriarte, 2006) and with plot design standards for many national forest inventory programs (e.g. Woudenberg et al., 2010).

Within the stand, neighborhoods are tended or regenerated over periodic harvest entries (say, every ten years). At each entry, any trees within the stand may be harvested, thereby generating a stream of harvest revenue, or retained and thereby determining the structure of each residual neighborhood and controlling each tree's growth over the subsequent period. Assume that once the last tree in a neighborhood is cut, that neighborhood naturally (and costlessly) regenerates, independent of the age, composition, or structure of the other neighborhoods in the stand; until then, no regeneration can become established within that neighborhood. By construction, no silvicultural activities other than harvesting occur—no site preparation, no planting, no pruning, no fertilization, etc.

At the level of individual neighborhoods, the timing of each tree's removal is specified to maximize the discounted value of the cumulative harvest revenue and of the bare land value realized when the neighborhood is regenerated. The harvest schedule that maximizes the capitalized value of each neighborhood, independently, will necessarily maximize the value of the entire stand. The combination and arrangement of treatments across all neighborhoods at each entry constitute an optimal sequence of stand-level prescriptions. The resulting silvicultural system is thus wholly determined by the initial conditions of the stand.

The ecological structure of the stand at any point in time is observable and determined from the aggregated tree populations of all the unregenerated neighborhoods, the variability in density and composition between those neighborhoods, and the proportional area of each "vintage" of

regenerated neighborhoods. The most plausible outcome of implementing such a strategy would be an unbalanced, irregular silvicultural system, in which structure and demographics are varied within the stand and change over time. In theory, though, under the right initial conditions, this approach could result in an even-aged silvicultural system (if every neighborhood is regenerated during a single entry) or a balanced group selection system (if an equal proportion of neighborhoods are regenerated at each entry).

Consider a stand comprised of $N$ neighborhoods, each of some equal fixed area $A$. Because neighborhoods operate—and are optimized—independently of each other, it is sufficient for expositional purposes to describe the growth dynamics and decision mechanics of just one arbitrary neighborhood of the $N$ neighborhoods in the stand. The growth of tree $i \in \{1, \dots, n\}$ from time $t_0$ to $t_1$, is a function of its physiological attributes such as its bole size and crown dimensions; of the initial neighborhood-level competitive environment it resides in at time $t_0$, as controlled by the attributes of the trees neighboring it; and of the fixed site attributes that relate to tree growth processes[1].

Let $\Delta DBH_{i0}$ denote the forward periodic diameter increment of tree $i$ over the first modeling timestep, where $\Delta DBH_{i0} = DBH_{i1} - DBH_{i0} = \Delta DBH_{i0}(DBH_{i0}, CR_{i0}, BA_0, BAL_{i0}; SPP_i)$. $SPP$ is a categorical variable that denotes the species of tree $i$; $DBH$ denotes diameter at breast height, $DBH \in (0, \infty)$; $CR$ denotes live crown ratio (the ratio of the length of tree's photosynthetically active crown to its total height and a proxy measure for a tree's overall vigor and productive potential), $CR \in [0,1]$; $BA_0$ is the initial neighborhood-level basal area (a measure of density):

$$BA_0 = \sum_{i=1}^{n} \left( {DBH_{i0}}^2 \frac{\pi}{4} A^{-1} \right) \tag{1}$$

and $BAL_{i0}$ is the initial overtopping basal area (i.e. basal area of larger trees), relative to tree $i$:

$$BAL_{i0} = \sum_{j=1}^{n} \left( {DBH_{j0}}^2 \frac{\pi}{4} A^{-1} I\left(DBH_{j0} > DBH_{i0}\right) \right) \tag{2}$$

where $j$ is an index of all trees in the neighborhood population, $j \in \{1, \dots, n\}$, and $I$ is an identity function, ($I = 1$ if $DBH_{jt} > DBH_{it}$, $I = 0$ otherwise). Define $\Delta CR_{i0}$ analogously to $\Delta DBH_{i0}$.

Given the significant role natural mortality plays in a forest's development, optimization modeling should account for it explicitly. Let $\phi_{i0}$ denote tree $i$'s probability of survival over the first timestep, where $\phi(\cdot)$ is a function of the same factors that determine $\Delta DBH$ and $\Delta CR$: $\phi_{i0} = \phi_{i0}(DBH_{i0}, CR_{i0}, BA_0, BAL_{i0}; SPP_i)$.

In a dynamic model, the states of each tree $i$ evolve over successive timesteps, $t \in \{t_0, t_1, \dots, T\}, T \in [t_0, \infty)$. Expected growth and mortality functions for times $t > 0$ require modification to account for reduced stocking resulting from probabilistic natural mortality. Let $E[BA_{i\tau}]$ denote the expected

[1] As fixed exogenous attributes, these site-descriptive variables can be suppressed in the analytical notation that follows without any loss of generality; specific variables used for growth modeling are discussed in the Numberical simulation section.

basal area affecting the growth and mortality of tree $i$ from an arbitrary time $\tau$ to $\tau + 1$, conditional on tree $i$ having survived until time $\tau$:

$$E[BA_{i\tau}] = \left( {DBH_{i\tau}}^2 + \sum_{j=1, j \neq i}^{n} \left( \Phi_{j\tau} {DBH_{j\tau}}^2 \right) \right) \frac{\pi}{4} A^{-1} \tag{3}$$

and let $E[BAL_{i\tau}]$ denote expected overtopping basal area, similarly qualified:

$$E[BAL_{i\tau}] = \sum_{j=1}^{n} \left( \Phi_{j\tau} {DBH_{j\tau}}^2 \frac{\pi}{4} A^{-1} I\left(DBH_{j\tau} > DBH_{i\tau}\right) \right) \tag{4}$$

where $\Phi_{j\tau}$ denotes the cumulative probability of survival up to time $\tau$:

$$\Phi_{j\tau} = \prod_{t=0}^{\tau} \phi_{jt} \tag{5}$$

from discrete, individual-tree survival probabilities:

$$\phi_{it} = \phi_{it}(DBH_{it}, CR_{it}, E[BA_{it}], E[BAL_{it}]; SPP_i) \tag{6}$$

where the state of tree $i$ diameter and crown ratio in time $\tau$ is given by:

$$DBH_{i\tau} = DBH_{i0} + \sum_{t=0}^{\tau} \Delta DBH_{it} \tag{7}$$

$$CR_{i\tau} = CR_{i0} + \sum_{t=0}^{\tau} \Delta CR_{it} \tag{8}$$

and where general diameter increment and crown ratio change functions are similarly modified to account for expected cumulative survival:

$$\Delta DBH_{it} = \Delta DBH_{it}(DBH_{it}, CR_{it}, E[BA_{it}], E[BAL_{it}]; SPP_i) \tag{9}$$

$$\Delta CR_{it} = \Delta CR_{it}(DBH_{it}, CR_{it}, E[BA_{it}], E[BAL_{it}]; SPP_i) \tag{10}$$

The economic dimension of the individual-tree harvesting problem entails the choice, in each period, of which trees to harvest and which to retain, and the valuation of the resulting cash flows. Let $v_{it}$ denote the potential gross harvest revenue of tree $i$ at time $t$, such that $v_{it} = v_{it}(DBH_{it}, HT_{it}, CR_{it}; SPP_i, q_i)$ where $HT_{it}$ denotes tree height, which evolves according to a height growth function, $\Delta HT$, defined analogously to $\Delta DBH$ and $\Delta CR$, and where $q_i$ is a quality vector, $q_i = \{q_{i1}, q_{i2}, \dots, q_{ib_{\text{max}}}\}$, where $q_{ib}$ denotes the timber quality class of the $bth$ 'bolt' (i.e. discrete merchantable bole section, typically 2.5 m in length) in the stem of tree $i$ and $b_{\text{max}}$ denotes the bole from the upper-most feasibly merchandizable stem section. Quality class $q_{ib}$ is a fixed attribute of bolt $b$ of tree $i$ and specifies the coefficients for the function that relates unit price, $p_{itb}$, to individual-bolt volume, $f_{ibt}$, (for bolts of a fixed length) where $p_{itb} = p_{itb}(f_{itb}; SPP_i, q_{ib})$, and $p(\cdot)$ is an increasing, sigmoidal function in $f$ (see Foppert, 2022, Figure 1).

For bolts of a fixed length, individual-bolt volume is determined by the tree's $DBH$, the bolt's position in the bole, $b$, and the stem taper form of tree $i$, which is a function of its physiological attributes, such that $f_{itb} = f_{itb}(DBH_{it}, HT_{it}, CR_{it}; SPP_i, b)$. The total potential gross harvest revenue of an individual tree is:

$$v_{it} = \sum_{b=1}^{b_{\max}} [p_{itb} \cdot f_{itb}] \tag{11}$$

Let $c_{it}$ denote the potential cost of harvesting tree $i$ at time $t$. From a forest owner's perspective, harvesting costs are a function of the structure of the timber sale contract and can include a share of gross revenue, to incentivize efficient utilization by the harvesting contractor, and/or a per-piece or per-unit-volume component (Leffler and Rucker, 1991). Consider $c_{it}$ a linear combination of revenue- and volume-based compensation: $c_{it} = \lambda v_{it} + \rho f_{it}$, where $\lambda$ denotes a revenue sharing contract parameter, $\lambda \in [0,1]$; $\rho$ denotes a unit-volume cost rate, $\rho \in [0, \infty)$; and $f_{it} = \sum_{b=1}^{b_{\max}} f_{itb}$. Abstract from any job-level fixed costs, harvest costs influenced by stand- or job-level variables, or any variable costs of silvicultural implementation (see Discussion).

Let the binary variable $\chi_{it}$ operate as the control variable, such that tree $i$ is harvested in period $t$ if $\chi_{it} = 1$ and is retained through the subsequent period if $\chi_{it} = 0$. An $n$-dimensional neighborhood-level harvest vector, $\boldsymbol{h}$, specifies the timing of harvest for each tree $i$, such that $\boldsymbol{h} = \{h_1, h_2, \dots, h_n\},\ h_i \in \{0,1, \dots, T\}$. Define $\chi_{it}$ as $\chi_{it} = 1$ for $t = h_i$ and $\chi_{it} = 0\ \forall\ t \neq h_i$. Realized stumpage (i.e. net revenue), $s_{it}$, is thus given by:

$$s_{it} = \chi_{it}(v_{it} - c_{it}) \tag{12}$$

Define $\Phi_{kt} = 0\ \forall\ t > h_k$ to remove the influence of any tree $k$ on the neighborhood competitive environment following its harvest. The expected present value in time $t_0$ of realized stumpage from harvesting tree $i$ at time $t = h_i$ is given by:

$$u_i = \Phi_{ih_i} s_{ih_i} (1 + r)^{-h_i} \tag{13}$$

where $r$ is the per-period discount rate and, by assumption, is specified exogenously for all forestry projects. Let $U$ denote the cumulative neighborhood-level present value of expected future cashflows from the current growing stock, $U = \sum_{i=1}^{n} u_i$.

By assumption, a neighborhood will regenerate naturally following the harvest of the last tree from the initial cohort. Natural regeneration is a stochastic process, so the exact distribution of attributes among trees that initialized the previous cohort will not necessarily be replicated. Following the establishment of regeneration, the expected present value of the infinite series of rotations within the neighborhood's fixed area is thus independent of the harvest schedule $\boldsymbol{h}$ specified for the initial cohort (see Foppert [2019] for an extended discussion). This bare land value or *land expectation value* ($LEV$) can be assigned exogenously or may be derived numerically if the outcome of regeneration, in expectation, is known. In either case, the solution to the optimization problem for the initial neighborhood relies on a fixed value of $LEV$ independent of the choice of harvest schedule. Here, we outline a method for solving for $LEV$ explicitly by representing regeneration over a single neighborhood.

Assume that the expected structure and attributes of the regenerated cohort is known. Populate a hypothetical neighborhood with trees such that the distribution of species, quality, $DBH$, $CR$, and $HT$ within the neighborhood correspond to the expected distribution of a regenerated neighborhood at the close of the stand establishment phase. Model the development of that neighborhood forward according to Equations 3–11. Denote the present value of the expected cashflows from the first rotation in the representative regenerated neighborhood by $\breve{U} = \breve{U}(\boldsymbol{h})$. Define $\breve{T}$ such that $\breve{T}(\boldsymbol{h}) = max\{h_1, h_2, \dots, h_n\}$ for any specified harvest vector. The maximum value of an infinite series of repeated rotations (see Supplementary information) is given by:

$$LEV = \max_{\boldsymbol{h}} \left[ \frac{\breve{U}(\boldsymbol{h})}{1 - \frac{1}{(1+r)^{\breve{T}(\boldsymbol{h})}}} \right] \tag{14}$$

Having defined $LEV$, the general silvicultural optimization problem for any initial neighborhood population can be stated as:

$$\max_{\boldsymbol{h}} \left[ U(\boldsymbol{h}) + \frac{LEV}{(1+r)^{T(\boldsymbol{h})}} \right] \tag{15}$$

Specifying harvest vectors independently across all the neighborhoods in a stand results in an unconstrained (often irregular) age class structure likely to evolve over time.

*Numerical simulation*

To illustrate the theoretical approach described above, we modeled optimal cutting schedules for three different northern hardwood stands (described in detail in Section 3), one constructed synthetically and two real stands inventoried in the field. For all cases, individual-tree data were represented over 7.32 m radius fixed-area plots (0.017 ha), following the design of US Forest Service Forest Inventory and Analysis (FIA) subplots (Woudenberg et al., 2010), treating each plot as a discrete neighborhood. For the empirical case studies a systematic sample of plots was taken and species, $DBH$ (measured in inches, converted to centimeters), $CR$ (estimated to the nearest 10%-class), and quality assessments for each potentially-merchantable 2.5 m bole section were recorded for every tree within each plot. Bole sections were evaluated for *potential* log grade, irrespective of current diameter (see Demchik et al., 2018). For the hypothetical stand, all of the above individual tree attributes were synthesized to produce a plot with the targeted structure and composition, as described in sub-section 3.1. All analysis was done in the R programming language (R Core Team, 2022).

Prices were estimated for each bole section of each tree following the methods described in Foppert (2022). A relative price factor ($RPF$) relates the projected unit price of the subject log section to the price of a reference grade, such as a #2 sawlog. For a given species group and quality class, the small-end diameter inside bark ($dib$) of a log prescribes $RPF$ according to the sigmoidal function:

$$RPF = \frac{\beta_0}{1 + exp\left[\frac{-\beta_1}{\beta_0}(dib - \beta_2)\right]} + \beta_3 \tag{16}$$

Note that $RPF$ is a unitless factor.

$RPF$ curves were fitted for three hardwood species groups, with groupings based on historic price performance: high-value species, including sugar maple (*Acer saccharum*), black cherry (*Prunus serotina*), and yellow birch (*Betula allegeniensis*); mid-value species, including red maple (*Acer rubrum*), white ash (*Fraxinus americana*), and paper birch (*Betula papyrifera*); and low-value species including aspen (*Populus* spp.) and American beech (*Fagus grandifolia*). $RPF$ curves were estimated from log price data from the Indiana Forest Products Price Report[2] from 1957-2019. Log prices across grades were referenced to #2 sawlog prices and plotted along the grade-limiting $dib$ values for potential veneer (4 clear faces [cf]), sawtimber (1-3 cf), and pallet/tie (0 cf) quality classes. For each species group and quality class, $RPF$-function coefficients were fitted to minimize residual squared errors. Table 1 presents $RPF$-function coefficients for each species group and quality class.

| Species group | Veneer class | | | | Sawtimber class | | | | Pallet/tie class | | | |
|---|---|---|---|---|---|---|---|---|---|---|---|---|
| | $\beta_0$ | $\beta_1$ | $\beta_2$ | $\beta_3$ | $\beta_0$ | $\beta_1$ | $\beta_2$ | $\beta_3$ | $\beta_0$ | $\beta_1$ | $\beta_2$ | $\beta_3$ |
| *High-value* | 3.746 | 1.788 | 14.495 | 0.563 | 1.485 | 1.032 | 12.311 | 0.563 | 0.203 | 0.144 | 6.261 | 0.501 |
| *Mid-value* | – | – | – | – | 0.884 | 0.629 | 12.379 | 0.759 | 0.041 | 0.064 | 4.583 | 0.759 |
| *Low-value* | – | – | – | – | 0.366 | 0.293 | 12.945 | 0.936 | 0.059 | 0.012 | 13.145 | 0.936 |

**Table 1.** RPF-function coefficients, by species group and quality class.

We calculated $dib$ at the top of each bole section from Westfall and Scott's (2010) taper equations. Roadside prices were calculated for individual trees in their specified harvest year from quality assessments, $dib$, and $RPF$ values of all merchantable log sections. Reference prices (#2 sawlog) were assigned to each individual species from an average of advertised local sawmill price sheets (Table 2). Prices were reported in units of U.S. dollars per thousand board feet (MBF)[3] and were assumed to remain constant, in real terms, over the simulation horizon.

| Species | Reference price |
|---|---|
| Ash | $400 |
| Aspen | $170 |
| Beech | $190 |
| Black cherry | $450 |
| Paper birch | $320 |
| Red maple | $400 |
| Sugar maple | $550 |
| Yellow birch | $450 |

**Table 2.** Reference prices (#2 sawlog), by species.

Harvesting costs for log products (i.e. veneer, sawtimber, and pallet logs) were calculated per cord and modeled as:

[2] Indiana imports a substantial volume of hardwood sawlogs from across the northeast and upper Midwest and the Indiana Forest Products Price Reports consists of the longest and most complete record of delivered sawlog prices; recent reports are available at https://www.in.gov/dnr/forestry/forestry-publications-and-presentations/ and historic reports at https://docs.lib.purdue.edu/timber/.

[3] Measures of volume were converted between units at 1 MBF = 2 cords; for reference, 1 cord is equal to approximately 2.5 $m^3$.

$$c_{it} = \lambda v_{it} + \rho f_{it} \quad (17)$$

We assigned cost function parameters $\lambda$ = 40% and $\rho$ = \$36/cord and a fixed trucking rate of \$37.50 per cord, resulting in stumpage rates consistent with those observed in the region. We assigned fixed stumpage prices of \$5 per cord for aspen pulp and \$15 per cord for all other pulp-quality volume, and a fixed cost for precommercial thinning of \$1.50 per tree for all removed trees less than 15 cm in diameter. Future-period net revenues were discounted back to present value terms at a 3.5% real discount rate.

To simulate individual tree growth and neighborhood dynamics, we developed nonparametric, random forest models (Breiman, 2001) of annual tree diameter, crown ratio, and height increment, and of the periodic probability of tree survival, following the methods described in Maker and Foppert (2023). We developed these models for trees in the 36 county Northern Forest region of northern New York and New England, in the eastern United States, using data from 11,286 remeasured plots from the FIA database[4], which were established using the current national standard plot design (Woudenberg et al., 2010). Data were from 399,358 unique trees across 28 species or species groups, with $DBH$ ranging from 2.5-122.9 cm and averaging 17.0 cm. Plot basal area ranged from 0.5-121.9 $m^2ha^{-1}$ and averaged 33.4 $m^2ha^{-1}$.

We set aside 2,257 randomly selected plots (20%) for final testing and used data from the remaining 9,029 plots for model training, with the dataset split based on plots rather than individual trees to ensure independence. Tree-level features used for training were $SPP$, $DBH$, $CR$, and $BAL$; plot-level features were $BA$, site productivity class, latitude, longitude, and elevation. $\Delta DBH$, $\Delta CR$, and $\Delta HT$ models were trained in R with the ranger package (Wright and Ziegler, 2017) with the aim of minimizing root mean squared error (RMSE). For all these models, we used 50 regression trees and the "extratrees" split rule. The number of features considered for splitting at each node (mtry values) for $\Delta DBH$, $\Delta CR$, and $\Delta HT$ were three, four, and three, respectively. The minimum node size was four for $\Delta DBH$, and ten for both $\Delta CR$ and $\Delta HT$. Model performance statistics for $\Delta DBH$, $\Delta CR$, and $\Delta HT$ are presented in Table 3, below. In a comparison of nonparametric and parametric (nonlinear least squares) models of diameter increment developed from the same dataset used here, Maker and Foppert (2023) found that models performed similarly for common situations but that the nonparametric model was considerably more accurate at predicting the growth of larger diameter trees, and of trees at the tails of the distributions of $CR$, $BA$, and $BAL$.

| Model | Mean response | RMSE | MAE | Mean Error |
|---|---|---|---|---|
| $\Delta DBH$ | 0.244 | 0.155 | 0.109 | -0.003 |
| $\Delta CR$ | -0.35 | 1.83 | 1.38 | -0.007 |
| $\Delta HT$ | 13.716 | 28.773 | 21.458 | -0.122 |

**Table 3.** Diameter, crown ratio, and height increment model performance statistics; models predict annualized change in units of cm ($\Delta DBH$ and $\Delta HT$) or percentage points ($\Delta CR$).

A different model structure was required to predict probability of survival. Remeasurement intervals varied for plots in the FIA database (with a mean value of 5.1 years). We included the remeasurement interval as a predictor instead of annualizing the predictions. Survival responses are

4 https://apps.fs.usda.gov/fia/datamart/datamart.html, downloaded December 6, 2020

highly unbalanced, with many more trees surviving a given remeasurement interval than dying. We used a "random over-sampling examples" approach with the ROSE package in R (Lunardon et al., 2014) to create a balanced synthetic training dataset of 354,653 trees. Random over-sampling examples is a smoothed bootstrapping method that simultaneously oversamples the minority class (i.e. trees that died) and undersamples the majority class (i.e. trees that survived). We trained the model using the Rborist package (Seligman, 2022) configured with 50 trees, a minimum node size of 2, and a "predFixed" value (the actual number of predictors to test for a given split) of 7. The trained model was tested against a set-aside dataset representing 87,729 remeasured trees. The model had a kappa value of 0.275 and an area under the curve (AUC) of 0.717.

Neighborhood dynamics were simulated over five-year timesteps, with harvests restricted to alternate simulation timesteps (10-year intervals) beginning in Year 0. Harvest vectors, denoting the year of removal for each individual tree, were specified for all neighborhoods. To search for near-optimal harvest vectors, we employed the genoud evolutionary algorithm using Mebane and Sekhon's (2011) rgenoud package. Genoud is a metaheuristic, global optimizer that can accommodate complex problems with multiple local maxima and integer solutions (Mebane and Sekhon, 2011). The algorithm takes a given population of potential solutions and evolves them over multiple generations with reproductive strategies that favor higher fitness solutions (i.e. those that generate a higher economic return), iteratively approaching a near-optimal solution. For each neighborhood, we initialized the algorithm with a population of 50 potential solutions (harvest vectors) and allowed it to evolve for up to 70 generations to search for the optimal harvest vector according to Equations 14–15.

## Case study descriptions

We modeled three different stands representing a variety of structural conditions observed across northern hardwood forests. Case Study 1 was constructed synthetically to represent the expected composition and structure of a regenerated neighborhood 50 years after establishment. Case Studies 2 and 3 analyzed real stands located in the Adirondack region of northern New York, USA, representing a managed, uneven-aged stand and a mature, unmanaged stand, respectively. Figure 1 illustrates the initial diameter distributions of the three case study stands.

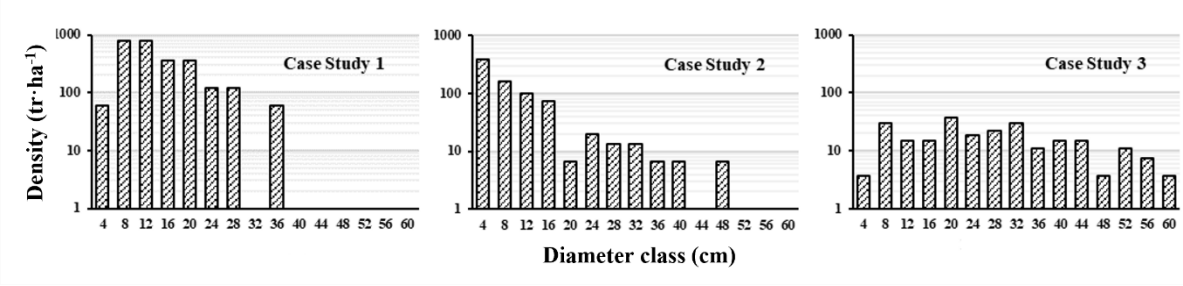


**Figure 1.** Case study initial diameter distributions (logarithmic scale).

The optimized cutting regime for Case Study 1 maximized the present value of identical, infinitely-repeated rotations (Equation 14). That value then served as $LEV$ in Equation 15 for the optimization of the empirical case study stands. For all optimizations, we simulated growth over five-year timesteps using the random forest models described in the Numerical simulation section. Removals were limited to alternate timesteps, beginning in Year 0, corresponding to ten-year cutting cycles. The subsections below provide detailed descriptions of each of the three case studies.

Qualitative information on the empirical stands was obtained from personal communication with the current owners and recent forest managers.

*Case Study 1 – Mid-rotation, even-aged*

We synthesized a representative 50-year-old regenerated neighborhood in three steps. First, we populated a 30-year-old neighborhood with composition and density matching Marquis's (1967) study of clearcutting in the White Mountains of New Hampshire. The granitic soils on that study site are similar to those in the Adirondacks. Marquis's (1967) observed species distributions (30% American beech, 29% sugar maple, 12% yellow birch) and stand density of 6,541 tr·ha$^{-1}$ are also consistent with local experience of regeneration on productive hardwood sites. We drew $DBH$ values from species-specific lognormal distributions fit to Marquis's (1967) reported mean values and randomly assigned $CR$ and $HT$ values from species-specific normal distributions derived from analysis of filtered FIA data. Quality scores for individual bolt sections were randomly assigned from the quality score distributions, by species group, observed from empirical assessments in Adirondack hardwood stands (Table 4).

| | Bolt | Veneer | Sawtimber | Pallet | Pulp |
|---|---|---|---|---|---|
| **Maple** | 1st | 28% | 51% | 10% | 11% |
| | 2nd | 11% | 65% | 14% | 10% |
| | 3rd | 1% | 40% | 30% | 30% |
| **Birch** | 1st | 48% | 33% | 7% | 13% |
| | 2nd | 27% | 40% | 14% | 19% |
| | 3rd | 1% | 40% | 19% | 41% |
| **Beech** | 1st | 0% | 5% | 48% | 47% |
| | 2nd | 0% | 3% | 42% | 55% |
| | 3rd | 0% | 0% | 24% | 76% |

**Table 4.** Quality score distributions of key species for hypothetical even-aged northern hardwood stand.

Second, we simulated the neighborhood dynamics from age 30 to age 50 absent any harvesting. The initialized age-30 population was grown forward in five-year timesteps, following the growth simulation methods described in Section 2.1. This resulted in a neighborhood population with modified age-50 $DBH$, $CR$, and $HT$ attributes and predicted cumulative probability of survival values for each tree.

Third, the neighborhood population was reduced to account for stochastic natural mortality. We assigned a random draw from a uniform distribution [0,1] to each tree and removed any tree for which the drawn value exceeded its age-50 cumulative survival probability. To avoid bias or arbitrariness in the results of the random draw, values were redrawn over 1,000 realizations, resulting in 1,000 unique age-50 tree lists. These realizations were filtered to exclude those with neighborhood-level stocking more or less than 5% of mean basal area across all 1,000 realizations. From that restricted set, we selected the tree list that most closely matched the distribution of veneer and sawtimber quality scores over the first two bolts for sugar maple and yellow birch from Table 4.

The resulting neighborhood contained 45 trees (2,677 tr·ha$^{-1}$). Mean $DBH$ was 14.2 cm within a range from 5.8-34.3 cm. The harvest schedule was optimized to maximize $LEV$, following Equation

14, for the market and financial parameters specified in Section 2.2. The value of $\breve{T}$ in Equation 14 (i.e. the rotation age) is defined as the age (not the simulation year) at which the last tree was harvested. This value is a function of the specified harvest vector and was unconstrained in the optimization.

*Case Study 2 – Managed, uneven-aged*

The first empirical case study stand is located on land owned by Lincoln Brook Timber Company in the Town of St. Armand, Essex County, New York. Stand 8 of the Pigeon Roost Lot is 24 ha in a mid-slope position on a moderately productive, northwest-facing granitic till hillside formed of bouldery, fine sandy loams (Beckett, Skerry, and Adirondack soil series). Elevations range from approximately 550-580 m.a.s.l. The stand was likely cleared for charcoal production in the late 19$^{th}$ century and regenerated as a primarily even-aged hardwood stand around that time. It was cut intermittently in the 20$^{th}$ century, including harvests in the 1950s and 1980s that led to the establishment of distinct cohorts. Most of the stand only suffered moderate damage in the 1998 ice storm, though the paper birch component (which was then 110-120 years old) was more severely damaged. The stand was lightly cut in 2000 to salvage storm damaged trees and harvest sawtimber deemed mature by the forester administering the timber sale. Lincoln Brook Timber Company acquired the tract containing this stand in 2003 and in the winter of 2016/2017 implemented a single-tree selection harvest under the planning and supervision of an experienced forester. The initial conditions for simulation and optimization were obtained from data from nine sample plots collected in November 2020. Sugar maple currently accounts for 44% of stand basal area, followed by black cherry (20%), American beech (18%), red maple (11%) and other associates. Optimal harvest vectors, dictating both the pattern of tending and the timing of regeneration within each neighborhood, were specified independently for each of the nine neighborhood plots according to Equation 15.

*Case Study 3 – Mature, unmanaged*

The second empirical case study stand is located in the Lot 57 Operational Unit of the Paul Smith's College Forest, in the Town of Brighton, Franklin County, New York. The 30-ha stand occupies a similar site as Case Study 2: mid-slope on a granitic till hillside (Beckett and Beckett-Tumbridge complex soils), with elevations from 530-570 m.a.s.l. Unlike the Lincoln Brook Timber tract, the Lot 57 Unit of the College Forest does not have well-developed road access. This stand has been unmanaged since at least the mid-1900s. Some earlier logging may have occurred but could only have been light, opportunistic cutting. Many trees in the stand predate the area's settlement in the late 1800's. Trees of different ages are present, but the majority of trees are over 100 years old and the canopy is mostly closed. Composition is typical for an older northern hardwood stand. Sugar maple accounts for 57% of stand basal area, and yellow birch, red maple, and American beech each account for around 12%. Timber quality is variable, but high-quality stems are present across size classes. An inventory of 16 sample plots in April 2021 provided the initial state for simulation and optimization. Removals from these 16 neighborhoods were independently optimized following Equation 15.

## Results

*Case Study 1 – Mid-rotation, even-aged*

The optimal harvest schedule for the simulated even-aged neighborhood was projected to generate an $LEV$ of \$562 ha$^{-1}$ over a 170-year rotation. Figure 2 illustrates the evolution of projected neighborhood-level stocking and associated cashflows.

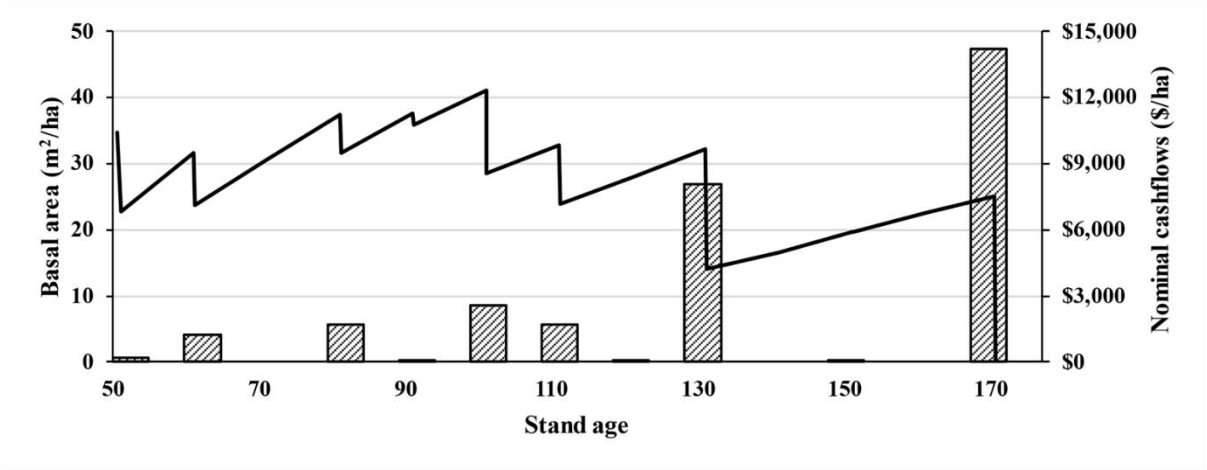


**Figure 2.** Simulated optimal stocking path (solid line) and undiscounted cashflow schedule (shaded bars, secondary axis) for hypothetical even-aged northern hardwood stand.

Tending began at the specified start of the optimization period. The first entry brought stand basal area (stems ≥ 14 cm) from 35 m$^2$ha$^{-1}$ to 23 m$^2$ha$^{-1}$. Removals in the first entry were concentrated among poorer quality stems (Table 5) distributed across intermediate size classes (Figure 3, left box). Subsequent tending maintained expected basal area within a range of approximately 25-40 m$^2$ha$^{-1}$.

| Stand age | Harvested | | Retained | |
|---|---|---|---|---|
| | *Mean* | *Max* | *Mean* | *Max* |
| **50** | \$0.52 | \$0.90 | \$0.63 | \$11.00 |
| **60** | \$6.85 | \$20.08 | \$0.62 | \$7.97 |
| **70** | \$0.00 | \$0.00 | \$1.20 | \$15.95 |
| **80** | \$14.37 | \$28.67 | \$1.40 | \$15.39 |
| **90** | \$0.99 | \$0.99 | \$2.71 | \$26.20 |
| **100** | \$21.70 | \$39.75 | \$4.00 | \$20.05 |
| **110** | \$14.46 | \$28.75 | \$8.19 | \$37.86 |
| **120** | -- | -- | \$15.72 | \$65.83 |
| **130** | \$67.73 | \$93.50 | \$4.92 | \$10.92 |
| **140** | -- | -- | \$9.60 | \$23.78 |
| **150** | -- | -- | \$18.65 | \$49.37 |
| **160** | -- | -- | \$32.39 | \$94.00 |
| **170** | \$59.71 | \$143.97 | -- | -- |

**Table 5.** Mean and maximum expected values per tree harvested or retained, hypothetical even-aged northern hardwood stand.

Thinnings between ages 50 and 130 employed a combination of methods. Crown-thinning-type treatments removed poorer-quality stems from the upper half of the diameter distributions, but a strategy consistent with dominant thinning (a.k.a. selection thinning) was observed at times. Beginning in year 80, high-quality red maple stems were removed from overtopping positions as they

reached diameters around 40-50 cm, as were good-quality (but not premium) yellow birch at around 30-40 cm (Figure 3, center box). At age 130, a final thinning removed good-quality red maple and yellow birch (40-50 cm) overtopping or competing with mostly premium-quality sugar maple and yellow birch. The residual stand was then free to grow, with an expected residual basal area of 14 $m^2ha^{-1}$. No removals occurred from years 130-170 when the remaining growing stock reached diameters around 50 cm and a final harvest brought the rotation to a close.

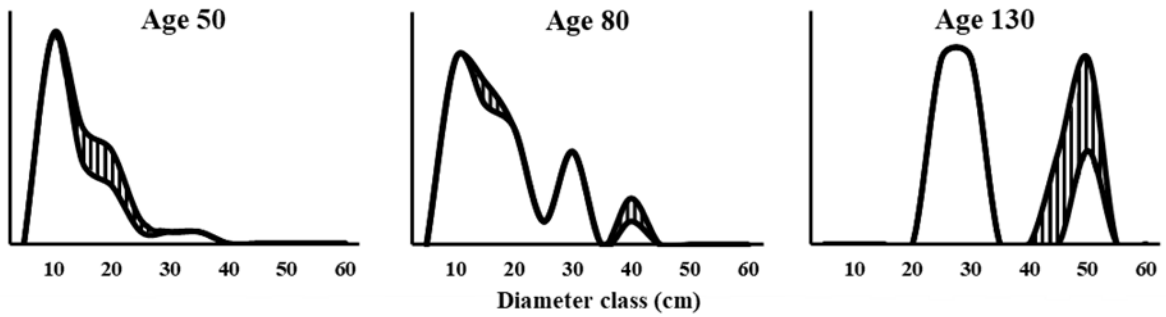


**Figure 3.** Simulated diameter distributions at selected mid-rotation entries along the optimal thinning schedule for the hypothetical even-aged northern hardwood stand; y-axis: relative size-class abundance (smoothed); hashed areas represent removals.

*Case Study 2 – Managed, uneven-aged stand*

The optimal harvest schedule generated discounted cashflows, inclusive of discounted neighborhood-level $LEV$ realizations, of \$2,761 $ha^{-1}$. Subtracting from this value the initial liquidation value (i.e. initial standing timber value plus stand-wide $LEV$) results in excess returns of \$573 $ha^{-1}$, a 26.2% premium over liquidation. Stand level cashflows are shown in Figure 4.

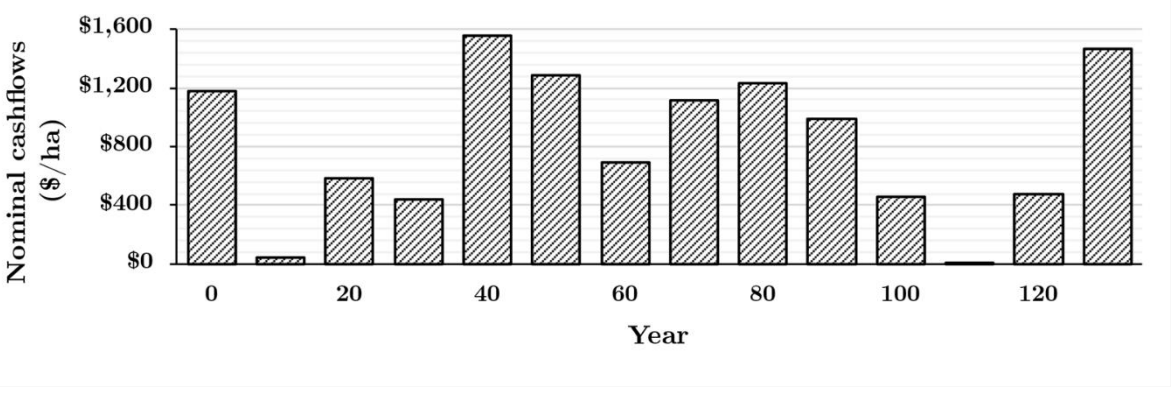


**Figure 4.** Optimized cashflow schedule, Lincoln Brook Timber Company, Pigeon Roost Lot, Stand 8.

Regeneration treatments among neighborhoods began in the first period and proceeded irregularly over 130 years. No regeneration treatments occurred in years 10, 30, 50, 70, 80, or 100-120; harvests in years 0, 20, 40, and 60 regenerated around 11% of the total stand area during each entry; one-third of the stand area was regenerated in year 90; and the remainder of the stand was regenerated in year 130.

Over the full simulation period, basal area of unregenerated neighborhoods averaged 14.5 $m^2ha^{-1}$, ranging at the stand level from a high of 19.7 $m^2ha^{-1}$ in year 40 to a low of 8.7 $m^2ha^{-1}$ following the entry in year 80. Naturally, stocking varied more widely at the individual-neighborhood level, ranging from 3.8-33.4 $m^2ha^{-1}$ with a standard deviation of 6.5 $m^2ha^{-1}$ around the mean of 14.5 $m^2ha^{-1}$.

As with Case Study 1, a variety of patterns of within-neighborhood removals were observed. Though these removals do not represent specific silvicultural thinning methods, *per se*, they corresponded closely to the patterns of removal prescribed by crown and dominant thinning methods (Ashton and Kelty, 2018).

*Case Study 3 – Mature, unmanaged*

Optimal harvesting generated capitalized value (inclusive of $LEV$ realizations) of \$5,258 $ha^{-1}$. Compared to a strategy of uniform liquidation and regeneration, this harvest schedule generated excess returns of \$228 $ha^{-1}$. A variety of tending patterns were observed and, as with Case Studies 1 and 2, target diameters were generally around 30-40 cm for mid-quality stems and 50 cm for the highest quality sugar maple and yellow birch stems.

The timing of regeneration treatments varied across the stand. 50% of neighborhoods were regenerated in the first entry. Regeneration of the remaining neighborhoods unfolded in an irregular pattern over the following 60 years; at no point did the stand approach a balanced age-class distribution (Figure 5).

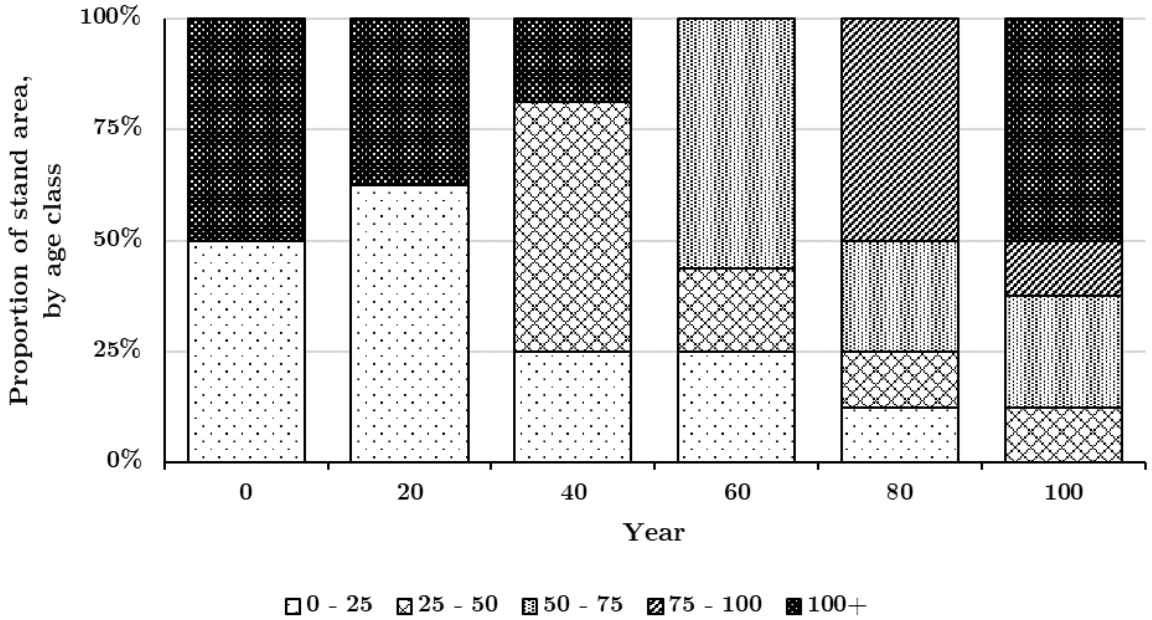


**Figure 5.** Evolution of projected (post-harvest) stand age-class structure, Paul Smith's College Forest, Lot 57; all initial growing stock assigned to 100+ age class, by assumption.

## Discussion

In all three case studies examined, the optimized harvest regimes required silviculturally sophisticated cutting patterns and resulted in ecologically complex stands. In the first case study,

optimal harvesting produced a rotation age of 170 years and target diameters in excess of 50 cm. Cutting strategies varied over the rotation, tailored to species-specific growth patterns and differentiated individual-tree vigor and quality. Mixed-species composition was maintained through the final entry.

The second case study examined a stand that began with high quality growing stock well-distributed across size classes and a spatial arrangement indicative of a professionally managed uneven-aged stand on path toward a desirably complex structure. Optimal management neither steered the stand away from that path nor rigidly bound it to a target structure. Within-neighborhood patterns of removal varied over time and across neighborhoods. At no point did the stand approach a steady distribution of size classes, age classes, or neighborhood- or stand-level stocking.

The third case study can be thought of as an exit strategy scenario. Given a mature stand, what would be the most profitable way to harvest the current growing stock and regenerate the stand? Here, we observed a 60-year process of distributed establishment cuts with attentive tending in the unregenerated matrix, resulting again in large target diameters, mixed species composition, and irregular spatial and demographic structure that never converged to a static equilibrium.

Our results present both similarities and differences with other published studies. Projected valuations were lower in our analysis than in other optimization studies (e.g. Fransson et al., 2020; Tahvonen et al. 2022), but the results in those studies are strongly affected by local factors, such as the significantly lower harvesting costs in the Nordic production systems relative to those in eastern North America. Other analyses conducted in similar northern hardwood forest types, including simulation studies (Saunders and Arseneault, 2013) and retrospective empirical analyses (Draper et al., 2021; Draper and Froese, 2021), broadly corroborate the results we obtained[5].

The results presented here also differ qualitatively from much of the pioneering work in economic-ecological optimization, which projected convergences toward steady-state systems sustained by regular, partial harvests (e.g. Tahvonen et al., 2010; Tahvonen and Rämö, 2016; Parkatti and Tahvonen 2020). Those studies, however, assumed spatial homogeneity at the stand-level, including uniformly distributed regeneration, and abstracted from quality differentiation at the tree-level. Such a framework leads much more naturally to steady-state results than would be expected from the quality-differentiated, spatially-irregular systems modeled here and in other hardwood tree-level optimization studies (Meilby and Nord-Larsen, 2011; Lohmander, 2019).

In that way, our approach builds on earlier work to develop irregular silvicultural strategies that apply multiple treatments within heterogeneous stands (Meek and Lussier, 2014; Labelle et al., 2018). But where Labelle et al.'s (2018) multi-treatment planning tool was explicitly "not meant to optimize or produce a heuristic solution based on financial returns" (p. 485), we showed that neighborhood-based, tree-level optimization offers a feasible (if still challenging) method for integrating economic and ecological modeling in such stands.

[5] Note, our results do project lower financial performance than in the papers cited above. Higher NPV values obtained by Saunders and Arseneault (2013) largely reflect their assumption of hardwood sawtimber stumpage real annual price growth of 4.5%, compared to our assumption of constant prices. Higher current timber values and projected future cashflows in the empirical studies largely stem from the significantly higher proportion of high-value sugar maple upper midwestern forests contain compared to the case studies we modeled.

As it relates to both thinning and regeneration, this framework can help bring rigor to the irregular silviculture deemed "seemingly less demanding and more informal as a silvicultural system" (Nyland et al., 2016, p. 518). Silviculturalists have long recognized the importance of thinning—Fernow (1911) gave credit for "the first good statement of the theory of thinnings" (p.67) to Berlepsch in 1761—but have also long struggled to bring it into a rigorous analytical framework. Recent progress in forest economics revealed how challenging the thinning question is. After providing a complete analytical treatment of the thinning problem, Coordes' (2014) concluded that "the viability of the scientific [i.e. economic] management of forest stands for profitable timber production is doubtful" (p.168) given the complexity of the solution.

Foppert (2019) argued that for both theoretical and numerical problems, the stand-level thinning problem can be broken up into smaller, neighborhood-scale problems and advocated for economists to borrow the gap model framework from forest ecology (e.g. Botkin et al., 1972; Shugart and West, 1980). Bugmann (2001) described the four "fundamental ecological abstractions that form the nucleus of gap models" (p. 261):

(1) *Spatial discretization* - Forest stands are composites of many small (100-1,000 $m^2$) patches

(2) *Within-patch horizontal homogeneity* – Resource competition and individual demographic processes are distance independent within patches

(3) *Size-structured competition* – Relative size, rather than spatial position, controls competition between individuals within patches

(4) *Patch-patch independence* – There are no interactions between patches

Representing a stand as a mosaic of independent neighborhoods reduces the complexity of a stand-scale, individual-tree thinning optimization problem by hundreds of orders of magnitude (Foppert, 2019). This approach preserves the heterogeneity of within-stand competitive environments and retains visibility of differential quality and growth potential between individuals without requiring spatially-explicit tree maps.

Beyond reducing the computational burden of the thinning problem, the gap model framework is useful for quantifying non-uniform regeneration strategies. Similar to the original applications of gap modeling in forest ecology, in quantitative silviculture and economic analysis it provides visibility of dynamic stand-level demographics. The neighborhood-based approach we presented here is also practical. From conventional, plot-based inventory data, it can provide decision support for developing irregular stand-level silvicultural prescriptions: Approximately what percentage of the stand area should be regenerated? Roughly, how much volume should be removed and from what size classes? In addition to guiding management, projected cash flows provide a basis for valuation of an otherwise hard-to-value silvicultural system and forest type.

Still, our model could benefit from refinement in several areas. Four opportunities stand out: mortality, harvesting costs and damage, price dynamics, and regeneration.

We addressed mortality by discounting each tree's competitive influence and its eventual harvest value by its cumulative survival probability in each period. This kept the model deterministic

and the optimization problem manageable while still accounting for mortality in evaluating cutting decisions and valuating the results. We consider this an improvement over other tree-level economic studies which abstract mortality out of their analysis (e.g. Meilby and Nord-Larsen, 2012; Lohmander, 2019; Foppert, 2022; Koster and Fuchs, 2022). A mechanistic representation of mortality will be increasingly important where environmental change is likely to change mortality dynamics (Anderegg et al., 2015)

Though our approach does better than just ignoring mortality, it is still problematic. It assumes that a tree with a 50% survival probability will exert an influence on its neighborhood competitive environment equivalent to half its basal area. "Expected basal area" perhaps makes sense in a tree-list model comprised of representative trees, but it challenges the logic of an individual-based model such as ours. A tree will either have survived and exert its full competitive influence or it will have died and exert none. To split the difference is to model an impossible scenario.

Sun et al. (2022) confronted this challenge, as well. It is common in tree-level simulations to draw random numbers [0, 1] and 'kill' a tree if its draw exceeds its survival probability (similar to the method we employed to construct the synthetic neighborhood in Section 3.1). In optimization settings, however, "repeated runs with the same decision variables should preferably give the same value for the objective function, which means that stochastic simulation should be avoided" (Sun et al., 2022, p. 4). Their approach was to assign a fixed random number to each tree, prior to optimization, rather than continuously re-drawing. Similar to our modeling strategy, this approach sidestepped the challenges of stochastic simulation, though theirs introduced an element of arbitrariness that would grow in significance with increasing differentiation by tree quality and vigor.

Future work could incorporate stochastic mortality into the adaptive control function optimization procedure Lohmander (2019) described, though this would require a nearly complete overhaul of the modeling strategy we used. For now, we consider our current approach a reasonable compromise between the high computational cost of a fully stochastic treatment of mortality and the bias of neglecting it altogether.

Stochastic prices are also well known to affect optimal harvesting strategies (e.g. Brazee and Mendelsohn, 1988; Platinga, 1998; Gong and Löfgren, 2007; Manley and Niquidet, 2017) but have been ignored in this study. Insulating decision making from price fluctuations results in under-valuation of forest assets. It also likely leads to mis-specified harvest schedules. As with mortality, future studies may have to abandon the convenience of modeling prices as deterministic (in this case, static) processes if they are to offer a fully formed solution to the problem at hand.

Our treatment of regeneration is also oversimplified but may be remediable without incorporating fully stochastic behavior into the model. The primary purposes of the tools we developed in this paper were to improve long-term valuation and to support near-term silvicultural decision making. In both cases, accounting for and planning around the *expected* outcomes of regeneration processes should not lead to distortions relative to an approach that evaluates the full distribution of potential outcomes. An improved model could treat regeneration as a deterministic dynamic process. Rather than using a simple binary process, in which a neighborhood regenerates always and only after the last tree is cut, different patterns of neighborhood-level residual growing stock (including, perhaps, time-lagged effects of structure over preceding timesteps) could result in the establishment of different cohorts that vary in their density and composition. Crucially, modeling

need not represent a new cohort as individually identified trees, so long as the effects of current neighborhood structure on future composition and density—and the resulting expected value of that regeneration—are quantified.

Harvest cost functions should also be more dynamic than the simple formula we employed. Ideally, they would account for job-level fixed costs and the stand-level attributes that affect variable operating costs (e.g. Germain et al., 2019; George et al., 2022). Unfortunately, such changes would substantially complicate our modeling approach, requiring a shift from independent neighborhood-level optimization to a significantly less efficient bi-level optimization approach similar to Tahvonen and Rämö (2016) or Sun et al. (2022).

Like harvesting costs, we also did not provide a full treatment of residual stand damage in this study. Harvesting damage and grade degradation can be estimated as a function of stand and job attributes (Wiedenbeck and Smith, 2019; Kizha et al., 2021). In the future, we could adjust quality scores to account for expected harvest damage, following the same mechanics as our current deterministic treatment of mortality. Short of a complete overhaul, there may be other more modest improvements to our harvest cost and damage functions that could be incorporated into the existing model structure. While future work should certainly explore these, we note that both the form and the values of the stumpage formula we used track with observed local timber sale contracts.

We also contend that for the setting of this study, the partial harvesting required by irregular silviculture does not entail categorically higher harvesting costs than conventional management. There is no reason to expect harvesting costs to differ between a system of irregular partial cutting and uniform partial cutting (say, following a conventional "B-line" thinning strategy). The functional factors that determine harvesting costs would be similar for both systems. Categorically higher harvest costs only emerge between partial harvesting and clearcutting (Soman et al., 2019). But selective cutting predominates in the Northern Forest (Canham et al., 2013; Belair and Ducey, 2018). True clearcuts are rare. In so much as the harvesting costs we used were consistent with those observed in practice, the relative inefficiency of partial harvesting was implicitly priced in.

Beyond our static treatment of harvesting costs and residual stand damage, this study also neglected the potential increase in management costs to implement such complicated prescriptions. Ashton and Kelty (2018) observed that "[t]he most profitable forest type is not necessarily the one with the greatest potential for growth or the one that can be used or harvested at lowest cost. One must also consider the silvicultural costs of growing the crop" (p. 13). Consideration of these "silvicultural costs" has generally been limited to the direct costs of production, such as site preparation, planting, pruning, etc. Analysis rarely takes account of the variable costs of implementation. Aside from acknowledging the potentially "higher treatment costs due to [their] more complex prescriptions," (Palik et al., 2021, p. 17) silviculturalists recommending irregular silviculture rarely evaluate (much less optimize) the costs and benefits of such complexity.

For their part, forest economists have generally been unhelpful in this setting, as well. The practical examples of management intensity economists analyze are almost always physical inputs such as increased planting density, improved genetics, or fertilization (e.g. Chang, 1983; Amacher et al., 1991; Halbritter and Deegen, 2015). The *decision* involves analysis of costly inputs, but the *decision making* is assumed to be perfect and costless. Irregular silviculture in complex, high-quality hardwood stands is different. There is a trade-off between the cost of an expert forester's time and attention,

on the one hand, and the sub-optimal marking decisions of a cheaper or more rushed forester, on the other. Clearly, much work remains in this area, but we argue our modeling strategy is well suited for exploring these questions.

## Conclusion

In this study, we incorporated advanced growth modeling and economic optimization methods into the neighborhood-based representation of forest stands. We modeled the growth of individual trees, subject to the structure of, and their relative positions in, the neighborhoods where they resided. Harvest decisions were similarly evaluated at the individual-tree-level. We used a global optimization algorithm to search over the universe of possible individual-tree cutting schedules within each neighborhood to find the exact cutting schedules that maximized financial returns. We specified intermediate tending and neighborhood-level end-of-rotation regeneration decisions independently across neighborhoods. Our approach was agnostic on silvicultural strategy: neighborhood-level composition and density, and stand-level demographics and spatial structure were all unconstrained. We optimized strictly on financial returns. Across three different case study northern hardwood stands, representing a range of initial stand structures, financially optimal harvesting was silviculturally sophisticated and lead to diverse, structurally and demographically complex stands with large-diameter trees well over a century old.

## Funding

This study received no specific funding.

## Acknowledgements

We acknowledge and sincerely appreciate the input and support provided by Martin Moog throughout the study's development, the constructive comments and suggestions of three anonymous reviewers, and the targeted feedback and generous encouragement of the handing editor and Editor-in-chief, Rubén Manso and Fabian Fassnacht.

## Conflict of interest statement

None declared.

## Data availability statement

Publicly available data underlying this article are available in the US Forest Service Forest Inventory and Analysis Database, at https://apps.fs.usda.gov/fia/datamart/datamart.html and in the Indiana Forest Products Price Reports, at https://docs.lib.purdue.edu/timber/ and https://www.in.gov/dnr/forestry/forestry-publications-and-presentations/; this article includes other data from private forest enterprises that cannot be shared publicly. The data will be shared on reasonable request to the corresponding author.

## References

Achim, A., Moreau, G., Coops, N.C., Axelson, J.N., Barrette, J., Bédard, S., Byrne, K.E., Caspersen, J., Dick, A.R., D'Orangeville, L. and Drolet, G., 2022. The changing culture of silviculture. *Forestry*, *95*(2), pp.143-152.

Amacher, G.S., Brazee, R.J. and Thomson, T.A., 1991. The effect of forest productivity taxes on timber stand investment and rotation length. *Forest Science*, *37*(4), pp.1099-1118.

Anderegg, W.R., Hicke, J.A., Fisher, R.A., Allen, C.D., Aukema, J., Bentz, B., Hood, S., Lichstein, J.W., Macalady, A.K., McDowell, N. and Pan, Y., 2015. Tree mortality from drought, insects, and their interactions in a changing climate. *New Phytologist*, *208*(3), pp.674-683.

Ashton, M.S. and Kelty, M.J., 2018. *The Practice of Silviculture: Applied Forest Ecology*. John Wiley & Sons.

Assmann E. 1970. *The Principles of Forest Yield Study: Studies in the Organic Production, Structure, Increment and Yield of Forest Stands.* Translated by S.H. Gardiner. Pergamon Press.

Assmuth, A., Rämö, J. and Tahvonen, O., 2021. Optimal carbon storage in mixed-species size-structured forests. *Environmental and Resource Economics*, *79*(2), pp.249-275.

Belair, E.P. and Ducey, M.J., 2018. Patterns in forest harvesting in New England and New York: Using FIA data to evaluate silvicultural outcomes. *Journal of Forestry*, *116*(3), pp.273-282.

Bettinger, P. and Tang, M., 2015. Tree-level harvest optimization for structure-based forest management based on the species mingling index. *Forests*, *6*(4), pp.1121-1144.

Botkin, D.B., Janak, J.F. and Wallis, J.R., 1972. Some ecological consequences of a computer model of forest growth. *The Journal of Ecology*, pp.849-872.

Brazee, R. and Mendelsohn, R., 1988. Timber harvesting with fluctuating prices. *Forest Science*, *34*(2), pp.359-372.

Breiman, L., 2001. Random Forests. *Machine Learning 45*, pp.5-32.

Bugmann, H., 2001. A review of forest gap models. *Climatic Change*, *51*(3), pp.259-305.

Canham, C.D. and Uriarte, M., 2006. Analysis of neighborhood dynamics of forest ecosystems using likelihood methods and modeling. *Ecological Applications*, *16*(1), pp.62-73.

Canham, C.D., Rogers, N. and Buchholz, T., 2013. Regional variation in forest harvest regimes in the northeastern United States. *Ecological Applications*, *23*(3), pp.515-522.

Chang, S.J., 1983. Rotation age, management intensity, and the economic factors of timber production: Do changes in stumpage price, interest rate, regeneration cost, and forest taxation matter? *Forest Science*, *29*(2), pp.267-277.

Coordes, R., 2014. Thinnings as unequal harvest ages in even-aged forest stands. *Forest Science*, *60*(4), pp.677-690.

D'Amato, A.W., Jokela, E.J., O'Hara, K.L. and Long, J.N., 2018. Silviculture in the United States: An amazing period of change over the past 30 years. *Journal of Forestry*, *116*(1), pp.55-67.

Das, A.J., Stephenson, N.L. and Davis, K.P., 2016. Why do trees die? Characterizing the drivers of background tree mortality. *Ecology*, *97*(10), pp.2616-2627.

Demchik, M.C., Conrad IV, J.L., Vokoun, M.M., Backes, B., Schellhaass, I. and Demchik, B.M., 2018. Crop tree release guidelines for 71-to 94-year-old oak stands based on height and financial maturity. *Journal of Forestry, 116(3)*, pp.217-221.

Dong, L., Bettinger, P. and Liu, Z., 2022. Optimizing neighborhood-based stand spatial structure: Four cases of boreal forests. *Forest Ecology and Management*, *506*, 119965.

Dong, L., Wei, H. and Liu, Z., 2020. Optimizing forest spatial structure with neighborhood-based indices: Four case studies from northeast China. *Forests*, *11*(4), p.413.

Draper, M.C. and Froese, R.E., 2021. Six decades of growth and yield and financial return in a silviculture experiment in northern hardwoods. *Forest Science*, *67*(5), pp.607-617.

Draper, M.C., Kern, C.C. and Froese, R.E., 2021. Growth, yield, and financial return through six decades of various management approaches in a second-growth northern hardwood forest. *Forest Ecology and Management*, *499*, p.119633.

Ek, A.R., Shifley, S.R., and Burk, T.E. 1988. *Forest Growth Modelling and Prediction*. USDA Forest Service General Technical Report NC-120.

Fernow, B.E., 1911. *A Brief History of Forestry in Europe, the United States and Other Countries*. University Press.

Foppert, J.D., 2019. Economic analysis at the neighborhood scale: Toward a new framework for forest valuation, management and research. *Allgemeine Forst- und Jagd-Zeitung*, *190*(11/12), pp.270-279.

Foppert, J.D., 2022. Worse off on purpose: An economic analysis of deliberate forest degradation. *Forest Ecology and Management*, *504*, 119771.

Franklin, J.F., Johnson, K.N. and Johnson, D.L., 2018. *Ecological Forest Management*. Waveland Press.

Fransson, P., Franklin, O., Lindroos, O., Nilsson, U. and Brännström, Å., 2020. A simulation-based approach to a near-optimal thinning strategy: Allowing harvesting times to be determined for individual trees. *Canadian Journal of Forest Research*, *50*(3), pp.320-331.

George, A.K., Kizha, A.R. and Kenefic, L., 2022. Timber harvesting on fragile ground and impacts of uncertainties in the operational costs. *International Journal of Forest Engineering*, *33*(1), pp.12-21.

Germain, R., Regula, J., Bick, S. and Zhang, L., 2019. Factors impacting logging costs: A case study in the Northeast, US. *The Forestry Chronicle*, *95*(1), pp.16-23.

Gong, P. and Löfgren, K.G., 2007. Market and welfare implications of the reservation price strategy for forest harvest decisions. *Journal of Forest Economics*, *13*(4), pp.217-243.

Graham, R.T. and Jain, T.B., 2005. Application of free selection in mixed forests of the inland northwestern United States. *Forest Ecology and management*, *209*(1-2), pp.131-145.

Halbritter, A. and Deegen, P., 2015. A combined economic analysis of optimal planting density, thinning and rotation for an even-aged forest stand. *Forest Policy and Economics*, *51*, pp.38-46.

764 Härtl, F., Hahn, A. and Knoke, T., 2010. Integrating neighbourhood effects in the calculation
765 of optimal final tree diameters. *Journal of Forest Economics*, *16*(3), pp.179-193.

766 Himes, A., Betts, M., Messier, C. and Seymour, R., 2022. Perspectives: Thirty years of triad
767 forestry, a critical clarification of theory and recommendations for implementation and
768 testing. *Forest Ecology and Management*, *510*, 120103.

769 Hyytiäinen, K. and Tahvonen, O., 2002. Economics of forest thinnings and rotation periods
770 for Finnish conifer cultures. *Scandinavian Journal of Forest Research*, *17*(3), pp.274-288.

771 Kant, S., Wang, S., Deegen, P., Hostettler, M., von Detten, R., Howard, T., Laband, D.,
772 Montgomery, C., Robert, N., Sekot, W. and Valatin, G., 2013. New frontiers of forest
773 economics. *Forest Policy and Economics*, *35*, pp.1-8.

774 Kizha, A.R., Nahor, E., Coogen, N., Louis, L.T. and George, A.K., 2021. Residual stand damage
775 under different harvesting methods and mitigation strategies. *Sustainability*, *13*(14), p.7641.

776 Koster, R. and Fuchs, J.M., 2022. Opportunity costs of growing space–an essential driver of
777 economical single-tree harvest decisions. *Forest Policy and Economics*, *135*, 102668.

778 Kuhn, M., 2008. Building predictive models in R using the caret package. *Journal of*
779 *Statistical Software*, *28*, pp.1-26.

780 Labelle, E.R., Pelletier, G. and Soucy, M., 2018. Developing and field testing a tool designed
781 to operationalize a multitreatment approach in hardwood-dominated stands in eastern
782 Canada. *Forests*, *9*(8), p.485.

783 Larsen, J.B., Angelstam, P., Bauhus, J., Carvalho, J.F., Diaci, J., Dobrowolska, D., Gazda, A.,
784 Gustafsson, L., Krumm, F., Knoke, T. and Konczal, A., 2022. Closer-to-Nature Forest
785 Management. *From Science to Policy 12*. European Forest Institute.

786 Leffler, K.B. and Rucker, R.R., 1991. Transactions costs and the efficient organization of
787 production: A study of timber-harvesting contracts. *Journal of Political Economy*, *99*(5),
788 pp.1060-1087.

789 Lohmander, P., 2019. Market Adaptive Control Function Optimization in Continuous Cover
790 Forest Management. *Iranian Journal of Management Studies*, *12*(3), pp.335-361.

791 Lunardon, N., Menardi, G. and Torelli, N., 2014. ROSE: a package for binary imbalanced
792 learning. *The R Journal*, *6*(1).

793 Lussier, J.M. and Meek, P., 2014. Managing heterogeneous stands using a multiple-
794 treatment irregular shelterwood method. *Journal of Forestry*, *112*(3), pp.287-295.

795 MacLeod, M. and Nagatsu, M., 2016. Model coupling in resource economics: Conditions for
796 effective interdisciplinary collaboration. *Philosophy of Science*, *83*(3), pp.412-433.

797 Mäkelä, A. and Valentine, H.T., 2020. *Models of Tree and Stand Dynamics*. Springer.

798 Maker, N.F. and Foppert, J.D. 2023. Nonparametric Individual-Tree Growth Models for the
799 Northern Forest. In: Kern, C.C., Dickinson, Y.L., eds. *Proceedings of the first biennial Northern*
800 *Hardwood Conference 2021: Bridging science and management for the future.* Gen. Tech.
801 Rep. NRS-P-211. Madison, WI: U.S. Department of Agriculture, Forest Service, Northern
802 Research Station: 83-95.

Manley, B. and Niquidet, K., 2017. How does real option value compare with Faustmann value when log prices follow fractional Brownian motion? *Forest Policy and Economics*, *85*(1), pp.76-84.

Marquis, D.A., 1967. *Clearcutting in northern Hardwoods: Results After 30 years*. Northeastern Forest Experiment Station, Forest Service, US Department of Agriculture.

Mebane Jr, W.R. and Sekhon, J.S., 2011. Genetic optimization using derivatives: the rgenoud package for R. *Journal of Statistical Software*, *42*, pp.1-26.

Meilby, H. and Nord-Larsen, T., 2012. Spatially explicit determination of individual tree target diameters in beech. *Forest Ecology and Management*, *270*, pp.291-301.

Miller, G.W., Stringer, J.W. and Mercker, D.C., 2007. Technical guide to crop tree release in hardwood forests. *Publication PB1774. Knoxville, TN: University of Tennessee Extension. 24 p. [Published with the University of Kentucky Cooperative Extension and Southern Regional Extension Forestry].*

Mitchell, K.J., 1975. Dynamics and simulated yield of Douglas fir. *Forest Science Monographs*, *17*, pp.1-39.

Newman, D.H., 2002. Forestry's golden rule and the development of the optimal forest rotation literature. *Journal of Forest Economics*, *8*(1), pp.5-27.

Nyland, R.D., Kenefic, L.S., Bohn, K.K. and Stout, S.L., 2016. *Silviculture: Concepts and Applications*. Waveland Press.

Pacala, S.W., Canham, C.D. and Silander Jr, J.A., 1993. Forest models defined by field measurements: I. The design of a northeastern forest simulator. *Canadian Journal of Forest Research*, *23*(10), pp.1980-1988.

Packalen, P., Pukkala, T. and Pascual, A., 2020. Combining spatial and economic criteria in tree-level harvest planning. *Forest Ecosystems*, *7*(1), pp.1-13.

Palik, B.J., D'Amato, A.W., Franklin, J.F. and Johnson, K.N., 2021. *Ecological Silviculture: Foundations and Applications*. Waveland Press.

Parkatti, V.P. and Tahvonen, O., 2020. Optimizing continuous cover and rotation forestry in mixed-species boreal forests. *Canadian Journal of Forest Research*, *50*(11), pp.1138-1151.

Pascual, A. and Guerra-Hernández, J., 2022. Spatial connectivity in tree-level decision-support models using mathematical optimization and individual tree mapping. *Forest Policy and Economics*, *139*, 102732.

Pascual, A., 2021. Multi-objective forest planning at tree-level combining mixed integer programming and airborne laser scanning. *Forest Ecology and Management*, *483*, 118714.

Pauwels, D., Lejeune, P. and Rondeux, J., 2007. A decision support system to simulate and compare silvicultural scenarios for pure even-aged larch stands. *Annals of Forest Science*, *64*(3), pp.345-353.

Plantinga, A.J., 1998. The optimal timber rotation: an option value approach. *Forest Science*, *44*(2), pp.192-202.

Pommerening, A. and Grabarnik, P., 2019. *Individual-based Methods in Forest Ecology and Management*. Springer.

R Core Team, 2020. *R: A Language and Environment for Statistical Computing*.

Raymond, P., Bédard, S., Roy, V., Larouche, C. and Tremblay, S., 2009. The irregular shelterwood system: review, classification, and potential application to forests affected by partial disturbances. *Journal of Forestry*, *107*(8), pp.405-413.

Schütz, J.P., 2002. Silvicultural tools to develop irregular and diverse forest structures. *Forestry*, *75*(4), pp.329-337.

Seligman, M. 2022. "Rborist." https://cran.r-project.org/web/packages/Rborist/Rborist.pdf.

Seymour, R.S., White, A.S. and Philip, G.D., 2002. Natural disturbance regimes in northeastern North America—evaluating silvicultural systems using natural scales and frequencies. *Forest Ecology and Management*, *155*(1-3), pp.357-367.

Shugart, H.H., 1984. *A Theory of Forest Dynamics. The Ecological Implications of Forest Succession Models*. Springer-Verlag.

Soman, H., Kizha, A.R. and Roth, B.E., 2019. Impacts of silvicultural prescriptions and implementation of best management practices on timber harvesting costs. *International Journal of Forest Engineering*, *30*(1), pp.14-25.

Stout, S.L. and Brose, P.H., 2014. The SILVAH saga: 40+ years of collaborative hardwood research and management highlight silviculture. *Journal of Forestry*, *112*(5), pp.434-439.

Saunders, M.R. and Arseneault, J.E., 2013. Potential yields and economic returns of natural disturbance-based silviculture: A case study from the Acadian Forest Ecosystem Research Program. *Journal of Forestry*, *111*(3), pp.175-185.

Sun, Y., Jin, X., Pukkala, T. and Li, F., 2022. Two-level optimization approach to tree-level forest planning. *Forest Ecosystems*, *9*, 100001.

Tahvonen, O. and Rämö, J., 2016. Optimality of continuous cover vs. clear-cut regimes in managing forest resources. *Canadian Journal of Forest Research*, *46*(7), pp.891-901.

Tahvonen, O. and Salo, S., 1999. Optimal forest rotation with in situ preferences. *Journal of Environmental Economics and Management*, *37*(1), pp.106-128.

Tahvonen, O., Pukkala, T., Laiho, O., Lähde, E. and Niinimäki, S., 2010. Optimal management of uneven-aged Norway spruce stands. *Forest ecology and management*, *260*(1), pp.106-115.

Tahvonen, O., Suominen, A., Malo, P., Viitasaari, L. and Parkatti, V.P., 2022. Optimizing high-dimensional stochastic forestry via reinforcement learning. *Journal of Economic Dynamics and Control*, *145*, p.104553.

Vauhkonen, J. and Pukkala, T., 2016. Selecting the trees to be harvested based on the relative value growth of the remaining trees. *European Journal of Forest Research*, *135*(3), pp.581-592.

Weiskittel, A.R., Hann, D.W., Kershaw Jr, J.A. and Vanclay, J.K., 2011. *Forest Growth and Yield Modeling*. John Wiley & Sons.

West, T., Sessions, J. and Strimbu, B.M., 2021. Heuristic optimization of thinning individual Douglas-fir. *Forests*. 12: 280.

Westfall, J.A. and Scott, C.T., 2010. Taper models for commercial tree species in the northeastern United States. *Forest Science*, *56*(6), pp.515-528.

Wiedenbeck, J. and Smith, K. T., 2018. Hardwood management, tree wound response, and wood product value. *The Forestry Chronicle*, *94*(3), pp.292-306.

Woudenberg, S.W., Conkling, B.L., O'Connell, B.M., LaPoint, E.B., Turner, J.A., Waddell, K.L., 2010. The Forest Inventory and Analysis Database: Database description and users manual version 4.0 for Phase 2. USDA Forest Service GTR-245.

Wright, M.N. and Ziegler, A., 2017. ranger: A fast implementation of random forests for high dimensional data in C++ and R. *Journal of Statistical Software*, *77*(i01).